Research Square

Preprints are preliminary reports that have not undergone peer review.
They should not be considered conclusive, used to inform clinical practice,
or referenced by the media as validated information.

Targeting the IL-8/CXCR1/2/NF-κB signaling axis suppresses metastatic progression in oral squamous cell carcinoma

Yuan-Feng Lin
Taipei Medical University
Sheng-Wei Feng
Taipei Medical University
Che-Hsuan Lin
Taipei Medical University
Hsiao-Wei Lu
Taipei Medical University
Yu-Hsien Kent Lin
North Shore Private Hospital
Shauh-Der Yeh
Taipei Medical University Hospital
I-Chun Lai
Taipei Veterans General Hospital
Chin-Beng Ho
Camillian Saint Mary's Hospital Luodong
Hsin-Lun Lee
leehsinlun@tmu.edu.tw

Taipei Medical University

Research Article

Keywords: Oral squamous cell carcinoma, lymph node metastasis, interleukin-8, IL-8/CXCR1/2/NF-κB signaling axis, predictive biomarker, therapeutic target

Posted Date: July 30th, 2026

DOI: https://doi.org/10.21203/rs.3.rs-10467902/v1

License: This work is licensed under a Creative Commons Attribution 4.0 International License.
Read Full License

Additional Declarations: No competing interests reported.

Abstract

Background

Oral squamous cell carcinoma (OSCC) is an aggressive malignancy with a high incidence of lymph node metastasis; however, the molecular mechanisms driving metastatic progression remain incompletely understood.

Methods

IL-8 expression profiles in OSCC were analyzed using The Cancer Genome Atlas (TCGA) and Gene Expression Omnibus (GEO) datasets and further validated in clinical specimens by RT-PCR. The functional role of IL-8 in metastatic progression was examined using Transwell migration assays and an orthotopic mouse model. NF-κB-mediated regulation of IL-8 transcription was evaluated using luciferase reporter assays.

Results

IL-8 expression was significantly elevated in OSCC tissues compared with normal tissues and was associated with unfavorable clinical outcomes. Ectopic expression of IL-8 in poorly metastatic Cal27 cells significantly enhanced migratory capacity, whereas IL-8 depletion in highly metastatic HSC3 cells reduced migration and lymph node metastatic dissemination in an orthotopic mouse model. Recombinant IL-8 restored the migratory ability of IL-8-deficient HSC3 cells, supporting a critical role of IL-8 in OSCC metastatic progression. Mechanistically, blockade of IL-8 signaling using the humanized anti-IL-8 antibody HuMax-IL8, the CXCR1/2 antagonist Reparixin, or NF-κB inhibitors significantly suppressed migration and NF-κB-dependent IL-8 transcription in OSCC cells. Furthermore, mutation of the NF-κB binding site within the IL-8 promoter abolished NF-κB-mediated transcriptional activation, demonstrating a functional IL-8/NF-κB positive feedback loop.

Conclusions

The IL-8/CXCR1/2/NF-κB signaling axis drives metastatic progression in OSCC and represents a potential prognostic biomarker and therapeutic target. Targeting this positive feedback loop may provide a promising strategy for patients with metastatic OSCC.

Introduction

Oral squamous cell carcinoma (OSCC) represents the predominant histological subtype of oral cancer, accounting for more than 90% of malignancies arising in the oral cavity. Despite advances in diagnostic and therapeutic strategies, OSCC remains an aggressive disease associated with substantial morbidity

and mortality, with only limited improvements in long-term survival outcomes over recent decades (El-Sakka et al. 2018). When detected at an early stage, the 5-year survival rate of OSCC patients can reach approximately 85%; however, this rate decreases to below 40% among patients presenting with distant metastasis (Abrahao et al. 2020; Speight et al. 2018). Current treatment approaches, including surgery, chemotherapy, and radiotherapy, remain the cornerstone of OSCC management, while emerging modalities such as intensity-modulated radiotherapy, proton therapy, immunotherapy, and targeted therapy have expanded therapeutic options (Gupta et al. 2025). Nevertheless, patients with advanced or refractory OSCC, particularly those with lymph node metastasis, continue to experience poor clinical outcomes, largely due to tumor recurrence, metastatic dissemination, and therapeutic resistance (Gamboa et al. 2020). Therefore, a better understanding of the molecular mechanisms driving OSCC metastasis and the identification of clinically relevant biomarkers and therapeutic targets are urgently required to improve patient prognosis.

Interleukin-8 (IL-8), also known as CXCL8, is a pro-inflammatory chemokine belonging to the CXC chemokine family and is produced by various cell types, including immune cells and tumor cells (Hedges et al. 2000). Aberrant IL-8 expression has been extensively implicated in tumor progression, therapeutic resistance, epithelial–mesenchymal transition (EMT), and metastatic dissemination across multiple cancer types (Sanmamed et al. 2017; Li et al. 2018; Jeong et al. 2025). In OSCC, elevated salivary IL-8 levels have been proposed as a potential biomarker for early detection (Kumar et al. 2025) and as a predictor of radiotherapeutic response (Sahibzada et al. 2017). Moreover, restoration of radiosensitivity and suppression of cancer stem-like properties in OSCC cells have been achieved through inhibition of IL-8 expression by microRNA let-7c (Peng et al. 2018). In addition, IL-8 blockade has been reported to attenuate migration, invasion, and cisplatin resistance in OSCC cells through regulation of the Akt/ERK–NF-κB signaling pathway (Bilusic et al. 2019). However, whether IL-8 and NF-κB establish a reciprocal regulatory circuit that sustains metastatic progression and therapeutic resistance in OSCC remains unclear. Furthermore, the therapeutic potential of targeting this signaling axis in metastatic OSCC has not been fully explored.

In the present study, we investigated the functional role of the IL-8/NF-κB feedback loop in regulating metastatic progression in OSCC. We demonstrate that IL-8 activates CXCR1/2-dependent NF-κB signaling, which subsequently reinforces IL-8 expression, establishing a positive feedback circuit that sustains the metastatic phenotype of OSCC cells. Pharmacological disruption of this signaling axis using the humanized anti-IL-8 monoclonal antibody HuMax-IL8, which has been evaluated in a phase I clinical trial (Bilusic et al. 2019), the CXCR1/2 antagonist Reparixin, or the NF-κB inhibitors BAY 11-7082 and SN50 significantly attenuated the migratory capacity of OSCC cells. Furthermore, IL-8 overexpression in poorly metastatic Cal27 cells enhanced lymph node metastatic dissemination, whereas IL-8 depletion in highly metastatic HSC3 cells markedly reduced lymph node metastasis in an orthotopic mouse model. Collectively, our findings identify the IL-8/CXCR1/2/NF-κB signaling axis as a critical regulator of OSCC metastatic progression and highlight its potential as a therapeutic target for patients with metastatic OSCC.

Materials and Methods

Collection of clinical datasets and human tissue specimens

Clinical annotation and transcriptomic datasets from patients with head and neck squamous cell carcinoma (HNSCC) were obtained from The Cancer Genome Atlas (TCGA) via the UCSC Xena platform (UCSC Xena, available at http://xena.ucsc.edu/welcome-to-ucsc-xena/). Gene expression data from oral squamous cell carcinoma (OSCC) patients were retrieved from the GSE42743 dataset in the Gene Expression Omnibus (GEO) database hosted by the National Center for Biotechnology Information (NCBI). Human OSCC tumor specimens and matched adjacent non-tumor tissues were obtained from the Taipei Medical University Biobank. The collection and use of clinical specimens were approved by the Institutional Review Board of Taipei Medical University (IRB No. N202204007) and performed in accordance with the Declaration of Helsinki.

Cell culture

Human oral squamous cell carcinoma (OSCC) cell lines Cal27 and HSC3 were obtained from the Japanese Collection of Research Bioresources (JCRB) Cell Bank. Cal27 cells were maintained in Dulbecco's Modified Eagle Medium (DMEM), whereas HSC3 cells were cultured in Minimum Essential Medium (MEM). The culture media were supplemented with 10% fetal bovine serum (FBS) for Cal27 cells and 5% fetal calf serum (FCS) plus 5% FBS for HSC3 cells, respectively. Cells were incubated at 37°C in a humidified atmosphere containing 5% CO_2. All media were supplemented with 1% Penicillin-Streptomycin solution, and all cell culture reagents were obtained from Gibco (Grand Island, NY, USA). The OSCC cell lines used in this study were routinely monitored for mycoplasma contamination and confirmed to be mycoplasma-free.

Reverse transcription PCR (RT-PCR) and quantitative real-time PCR (qPCR)

Total RNA was isolated from cultured cells using TRIzol reagent (Invitrogen) according to the manufacturer's instructions. Reverse transcription was performed using 5 μg of total RNA as the template with M-MLV reverse transcriptase (Invitrogen) to generate complementary DNA (cDNA). Conventional RT-PCR was subsequently conducted to evaluate IL-8 mRNA expression using specific primer pairs as follows: IL-8 forward, GAACTGAGAGTGATTGAGAGTGGACCAC; IL-8 reverse, GCAACCCTACAA CAGACCCACACAATAC; β-actin forward, AAGGATTCCTATGTGGGC; and β-actin reverse, CATCTCTTGCTCGAAGTC. For quantitative PCR analysis, cDNA samples were amplified using Power SYBR™ Green PCR Master Mix (Thermo Fisher) with gene-specific primers. The primer sequences were as follows: IL-8 forward, CTGCAGCTCTGTGTGAAGGTG; IL-8 reverse, GTGGTCCACTCTCAATCACTCTC; GAPDH forward, GGAAGGTGAAGGTCGGAGTCAACG; and GAPDH

reverse, AGCAGAGGGGGCAGAGATGATGAC. In conventional RT-PCR experiments, IL-8 expression was normalized to β-actin based on band intensity analysis. For qPCR assays, relative expression levels were normalized against GAPDH and calculated using the $2^{-\Delta\Delta Ct}$ method.

Gene set enrichment analysis (GSEA)

RNA-sequencing datasets from primary OSCC tumors and matched adjacent normal tissues available in The Cancer Genome Atlas (TCGA) were analyzed to identify genes differentially expressed between tumor and non-tumor samples. Differential expression results were ranked according to fold-change values to generate an ordered gene list for subsequent gene set enrichment analysis (GSEA). Pathway enrichment analysis was performed using the GSEA computational framework with the HALLMARK gene sets obtained from the Molecular Signatures Database (MSigDB; https://www.gsea-msigdb.org/gsea/msigdb; accessed January 1, 2022). Enrichment significance was evaluated based on normalized enrichment scores (NES) to identify biological processes and signaling pathways associated with OSCC progression.

Lentiviral-mediated IL-8 overexpression and silencing

Lentiviral vectors encoding IL-8 or the corresponding empty vector control, both carrying a puromycin resistance cassette, were obtained from Applied Biological Materials Inc. (Richmond, BC, Canada). Lentiviral constructs expressing nonspecific control shRNA (oligo sequence: CCGGACACTCGAGCACTTTTTG) or IL-8-targeting shRNAs (sh1: CAAGGAGTGCTAAAGAACTTA; sh2: CCGAACTTTAATTTCAGGAAT) were provided by the National RNAi Core Facility Platform (Taipei, Taiwan). For lentiviral transduction, cells seeded in 6-well plates were infected at approximately 50% confluence with lentiviral particles in complete medium containing 5 μg/mL polybrene (Santa Cruz). The infection was performed overnight at a multiplicity of infection (MOI) ranging from 2 to 10. Following transduction, stable cell populations expressing control or IL-8 shRNAs were established by puromycin selection (10 μg/mL for 24 h). The efficiency of IL-8 knockdown was subsequently verified by quantitative PCR using RNA extracted from puromycin-resistant cells.

Western blot analysis

Protein lysates prepared from the indicated experimental conditions were subjected to sodium dodecyl sulfate–polyacrylamide gel electrophoresis (SDS-PAGE). Following electrophoretic separation, proteins were transferred to polyvinylidene difluoride (PVDF) membranes. The membranes were blocked for 2 h at room temperature with either 5% bovine serum albumin (BSA) for detection of phosphorylated proteins or 5% nonfat milk prepared in Tris-buffered saline containing 0.1% Tween-20 (TBST) to reduce nonspecific antibody binding. After blocking, membranes were incubated with primary antibodies overnight at 4°C. The antibodies used included anti-phospho-NF-κB p65 (Ser536) (1:1000; #3033S, Cell Signaling Technology), anti-NF-κB p65 (1:1000; #6956S, Cell Signaling Technology), and anti-GAPDH

(1:1000; #2118S, Cell Signaling Technology). Membranes were subsequently washed extensively and incubated with appropriate horseradish peroxidase (HRP)-conjugated secondary antibodies for 1 h at room temperature. Immunoreactive bands were visualized using an enhanced chemiluminescence (ECL) detection system (Amersham Biosciences, GE Healthcare, Billerica, MA, USA).

Enzyme-linked immunosorbent assay (ELISA)

The concentration of secreted IL-8 protein in conditioned media collected from cultured cells was quantified using a commercially available human IL-8 enzyme-linked immunosorbent assay (ELISA) kit (R&D Systems, Minneapolis, MN, USA). The assay was performed according to the manufacturer's instructions, and IL-8 levels were determined based on the standard curve generated from recombinant IL-8 standards.

Cell migration assay

Cell motility was evaluated using a Boyden chamber-based migration assay (NeuroProbe, Gaithersburg, MD, USA) following the manufacturer's protocol. Briefly, the lower surface of an 8-μm pore size polycarbonate membrane (25 mm × 80 mm; NeuroProbe, USA) was coated with human fibronectin (10 μg; Sigma, MO, USA). The lower compartment was filled with conditioned medium containing 10% FBS as a chemoattractant. Cells (1.5×10^4) suspended in 50 μL of serum-reduced medium (0.1% FBS) were subsequently added to the upper chamber. After incubation for 4 h, cells remaining on the upper surface of the membrane were gently removed, and migrated cells attached to the lower membrane surface were fixed with 100% methanol and stained with 10% Giemsa solution (Merck, Germany) for 1 h. Migrated cells were quantified by microscopic examination. Each experiment was conducted in triplicate and independently repeated three times.

Plasmid construction and site-directed mutagenesis

The promoter region (~ 1 kb) of the human IL-8 gene was amplified from human genomic DNA using a touchdown PCR protocol (Han et al. 2004) with paired primers (forward: GTTGGAACCCAGATGCTCTTTCCA CTAAGC; reverse: GCTGTCTCTGAAAGTTTGTGCCTTA TGGAG). The PCR product was used as a template for a subsequent sticky-end PCR protocol (Zeng 1998) incorporating XhoI/HindIII restriction sites using two paired primers (#1: forward-TCGAGTTTCCACTAAGCATACAACTTTCC; reverse-TGC CTTATGGAGTGCTCCGG; #2: forward-GTTTCCACTAAGCATACAACTTTCC; reverse-AGCTT GCCTTATGGAGTGCTCCGG). PCR products were phosphorylated using T4 polynucleotide kinase (New England Biolabs, Ipswich, MA, USA) and subcloned upstream of the luciferase gene in the pGL4.10 vector (Promega, Madison, WI, USA). The construct was used as a template for site-directed mutagenesis targeting the NF-κB-binding element using paired primers (forward: TCATTATGTCAG AGGAGGTTTTACGATTTGCAACTGATGGCCCATCCCCTC; reverse: GAGGGGATGGGCCAT CAGTTGCAAATCGTAAAACCTCCTCTGACATAATGA). The mutation sites were

shown as underlined in the DNA sequences of paired primers. All constructs were validated by DNA sequencing to ensure sequence fidelity and correct orientation.

Luciferase reporter assay

NF-κB transcriptional activity was evaluated using a dual-luciferase reporter assay. The NF-κB-responsive firefly luciferase reporter vector was purchased from Promega, and pGL4.10-based reporter constructs were generated in this study. Cells seeded in 6-well plates were transiently cotransfected with Renilla luciferase plasmids as an internal control together with either NF-κB response element-containing firefly luciferase reporters or pGL4.10-derived constructs. After 24 h of transfection, cells were harvested and lysed for determination of luciferase activity using the Dual-Glo® Luciferase Assay System (Promega, Madison, WI, USA) according to the manufacturer's protocol. Firefly luciferase signals were normalized to the corresponding Renilla luciferase activity to calculate relative promoter activity.

Animal experiments

Advanced severe immunodeficiency (ASID) B6.129S4-Il2rgtm1Wjl/J mice were supplied by the National Laboratory Animal Center (Taiwan). All animal procedures were performed in accordance with institutional guidelines and were approved by the Institutional Animal Care and Use Committee of Taipei Medical University (IACUC approval No. LAC2023-0537). Luciferase-labeled OSCC cell derivatives were harvested, resuspended in phosphate-buffered saline (PBS), and adjusted to a concentration of 5×10^7 cells/mL. Following anesthesia, mice received orthotopic implantation of 20 μL cell suspensions into the buccal mucosa. Tumor progression and lymph node metastatic dissemination were evaluated weekly by bioluminescence imaging using an IVIS imaging system.

Statistical analysis

Statistical analyses were conducted using SPSS software version 17.0 (Informer Technologies, Roseau, Dominica). Survival outcomes were assessed using Kaplan–Meier analysis, and differences between survival curves were determined by the log-rank test. Comparisons of gene expression levels between clinical specimens were performed using Student's t-test or paired Student's t-test, as appropriate. The Friedman test was applied for analysis of nonparametric datasets. A two-sided p value of < 0.05 was considered statistically significant for all analyses.

Results

IL-8 is frequently upregulated in OSCC tumors and predicts unfavorable clinical outcomes

To investigate the clinical relevance of IL-8 in oral squamous cell carcinoma (OSCC), we first analyzed IL-8 transcript levels in primary tumors and normal tissues using multiple independent public datasets. Analysis of unpaired and paired OSCC specimens from The Cancer Genome Atlas (TCGA), GSE42743, and GSE213862 cohorts revealed that IL-8 mRNA expression was significantly elevated in tumor tissues

compared with matched or unmatched adjacent normal tissues ($p < 0.01$; Fig. 1A–C). Furthermore, IL-8 expression was markedly increased in OSCC tumors compared with normal oral tissues from healthy individuals in the GSE213862 and GSE25099 datasets (Fig. 1C, D). To further validate the bioinformatics findings, we examined IL-8 expression in an independent cohort consisting of 23 paired OSCC primary tumors and adjacent normal tissues collected from the Taipei Medical University (TMU) Biobank. Consistent with the public dataset analyses, RT-PCR analysis demonstrated a significant increase in IL-8 expression in tumor specimens compared with corresponding non-tumor tissues (Fig. 1E, F). We next evaluated the prognostic significance of IL-8 expression in OSCC patients. Kaplan–Meier survival analysis under the optimal cutoff condition demonstrated that patients with elevated IL-8 expression exhibited significantly poorer overall survival in both TCGA and GSE42743 cohorts (Fig. 1G). These findings indicate that IL-8 overexpression is a common molecular feature of OSCC and is associated with tumor progression and unfavorable clinical outcomes.

IL-8 expression is associated with metastatic signatures and enhances the migratory phenotype of OSCC cells

To identify molecular pathways associated with OSCC progression, we first compared transcriptomic profiles between primary tumors and adjacent normal tissues from TCGA OSCC patients. Principal component analysis (PCA) demonstrated a clear separation between tumor and non-tumor specimens, indicating distinct transcriptional landscapes in OSCC (Fig. 2A). Differentially expressed gene (DEG) analysis further revealed that IL-8 was significantly upregulated in OSCC tumors, showing an approximately three-fold increase in expression ($\log_2$ fold change = 1.61, $p = 3.65 \times 10^{-5}$) compared with adjacent normal tissues (Fig. 2B). Gene set enrichment analysis (GSEA) based on the identified DEGs showed significant enrichment of multiple cancer-associated pathways in OSCC tumors. Cell cycle-related signatures, including G2M_CHECKPOINT, E2F_TARGETS, and MITOTIC_SPINDLE, as well as metastasis-associated pathways, including EPITHELIAL_MESENCHYMAL_TRANSITION and APICAL_JUNCTION, were markedly activated. In addition, immune-related signaling represented by INTERFERON_ALPHA_RESPONSE was also enriched in OSCC tumors (Fig. 2C, D). Given the strong association between IL-8 expression and epithelial–mesenchymal transition (EMT), a critical event during metastatic dissemination, we investigated whether IL-8 levels were correlated with the migratory capacity of OSCC cells. Among the examined OSCC cell lines, poorly migratory Cal27 cells exhibited relatively low IL-8 secretion, whereas highly migratory HSC3 cells displayed elevated IL-8 production (Fig. 2E, F). Treatment with recombinant IL-8 significantly increased the migratory ability of Cal27 cells, whereas blockade of extracellular IL-8 using the humanized anti-IL-8 antibody HuMax-IL8 (Bilusic et al. 2019) markedly impaired HSC3 cell migration (Fig. 2H, I). To further establish the functional role of IL-8 in OSCC migration, IL-8 expression was genetically manipulated in Cal27 and HSC3 cells. Ectopic IL-8 expression in Cal27 cells enhanced IL-8 production and significantly promoted cell migration, whereas IL-8 depletion in HSC3 cells reduced IL-8 expression and suppressed migratory activity (Fig. 3A–F). Pharmacological inhibition of IL-8 signaling using HuMax-IL8 or the CXCR1/2 antagonist Reparixin further confirmed that disruption of IL-8 signaling significantly attenuated migration of IL-8-

overexpressing Cal27 cells in a dose-dependent manner (Fig. 3G). Conversely, supplementation with recombinant IL-8 effectively restored the migratory capacity of IL-8-silenced HSC3 cells (Fig. 3H). We next evaluated the impact of IL-8 expression on OSCC metastasis in an orthotopic mouse model. Forced IL-8 expression in Cal27 cells significantly enhanced tumor growth and distant lymph node metastasis, whereas IL-8 knockdown in HSC3 cells markedly reduced tumor progression and metastatic dissemination (Fig. 4A–F). These findings demonstrate that IL-8 functions as a critical driver of OSCC metastatic progression.

NF-κB activation is required for IL-8-induced migratory capacity of OSCC cells

Because NF-κB is a major transcriptional regulator of inflammatory cytokines, including IL-8, we investigated whether IL-8 signaling reciprocally regulates NF-κB activation in OSCC cells. In Cal27 cells, enforced IL-8 expression markedly increased NF-κB activation, as evidenced by elevated levels of phosphorylated NF-κB p65 and enhanced NF-κB transcriptional activity in luciferase reporter assays (Fig. 5A). Conversely, depletion of IL-8 in HSC3 cells significantly reduced both NF-κB phosphorylation and transcriptional activity (Fig. 5B). To further determine whether extracellular IL-8 signaling contributes to NF-κB activation, IL-8-overexpressing Cal27 cells were treated with HuMax-IL8 or Reparixin, an antagonist targeting IL-8 receptors CXCR1/2. Both approaches resulted in a dose-dependent reduction of NF-κB activation, including decreased phosphorylated NF-κB p65 levels and diminished NF-κB reporter activity (Fig. 5C). In contrast, supplementation with recombinant IL-8 restored NF-κB activation in IL-8-silenced HSC3 cells in a concentration-dependent manner (Fig. 5D). We next examined whether NF-κB activation is functionally required for IL-8-mediated migration. Pharmacological inhibition of NF-κB using BAY-11-7082 or SN50 significantly suppressed the migratory capacity of IL-8-overexpressing Cal27 cells and parental HSC3 cells in a dose-dependent manner (Fig. 5E, F). These findings demonstrate that IL-8 promotes OSCC cell migration through activation of NF-κB signaling, supporting the existence of an IL-8/NF-κB regulatory circuit that contributes to OSCC metastatic progression.

IL-8 and NF-κB establish a positive feedback loop to sustain OSCC progression

Previous studies have demonstrated that NF-κB directly binds to the IL-8 promoter and induces IL-8 transcription (Mizuno et al. 2022; Xu et al. 2014; Park et al. 2008; Oem et al. 2008). Based on these findings, we investigated whether disruption of the IL-8–CXCR1/2–NF-κB signaling cascade could attenuate IL-8 expression in OSCC cells. Pharmacological blockade of this signaling axis using HuMax-IL8, Reparixin, or NF-κB inhibitors (BAY-11-7082 and SN50) significantly reduced IL-8 mRNA expression (Fig. 6A) and extracellular IL-8 secretion (Fig. 6B) in IL-8-overexpressing Cal27 cells ($p < 0.01$). Similar inhibitory effects were observed in HSC3 cells (Fig. 6C, D). To further elucidate the molecular mechanism underlying NF-κB-dependent IL-8 regulation, *in silico* analysis identified a putative NF-κB binding motif within the IL-8 promoter region spanning − 82 to + 91 bp (Fig. 6E). We subsequently

established an IL-8 promoter-driven luciferase reporter system to evaluate NF-κB-mediated transcriptional regulation. Disruption of IL-8 signaling through HuMax-IL8, Reparixin, or NF-κB inhibition significantly suppressed IL-8 promoter activity in both IL-8-overexpressing Cal27 cells and HSC3 cells (Fig. 6F, G). Importantly, mutation of the predicted NF-κB binding site within the IL-8 promoter abolished reporter activity in HSC3 cells, confirming the critical role of this regulatory element in NF-κB-mediated IL-8 transcription (Fig. 6H). These findings demonstrate that IL-8 activates CXCR1/2-dependent NF-κB signaling, which subsequently reinforces IL-8 transcription, thereby establishing a positive feedback loop that sustains the metastatic phenotype of OSCC.

Discussion

Lymph node metastasis represents a major determinant of poor prognosis in patients with oral squamous cell carcinoma (OSCC); however, the molecular mechanisms driving metastatic dissemination remain incompletely understood. In this study, we identified the pro-inflammatory cytokine IL-8 as a critical mediator of OSCC metastasis. IL-8 expression was significantly elevated in OSCC tumors compared with adjacent normal tissues and was associated with aggressive tumor behavior and unfavorable clinical outcomes. Mechanistically, we demonstrated that IL-8 signaling through CXCR1/2 activates NF-κB, which subsequently enhances IL-8 transcription, establishing a positive feedback loop that maintains the metastatic phenotype of OSCC cells. Importantly, pharmacological disruption of this signaling circuit using the humanized IL-8-neutralizing antibody HuMax-IL8, the CXCR1/2 antagonist Reparixin, or NF-κB inhibitors BAY 11-7082 and SN50 effectively impaired the migratory and metastatic capacities of OSCC cells with elevated IL-8 expression (Fig. 7). These findings highlight IL-8 as a potential biomarker for identifying OSCC patients at increased risk of lymph node metastasis and provide a translational rationale for targeting the IL-8–CXCR1/2–NF-κB signaling axis as a therapeutic strategy for metastatic OSCC.

The existence of an IL-8/NF-κB positive feedback loop that enhances tumor invasiveness and cancer stem cell properties has been reported in intrahepatic cholangiocarcinoma (Song et al. 2025). In addition, our previous study demonstrated that activation of an IL-8/NF-κB feedback circuit contributes to a paclitaxel-sensitive but doxorubicin-resistant phenotype in triple-negative breast cancer (TNBC) (Lin et al. 2025). Although IL-8 and NF-κB have individually been implicated in promoting metastatic progression and therapeutic resistance in OSCC (Pu et al. 2021; Peng et al. 2016; Tamatani et al. 2004; Joshi et al. 2023), the functional interplay between these two signaling molecules in OSCC metastasis has remained largely unexplored. Here, we provide evidence that an IL-8/NF-κB positive feedback loop is established in OSCC and plays a critical role in sustaining the metastatic phenotype of OSCC cells. Future investigations are warranted to determine whether activation of this signaling circuit contributes to resistance against conventional therapies, including chemoradiotherapy, and whether pharmacological disruption of the IL-8/NF-κB axis can enhance treatment responses, such as paclitaxel sensitivity, in metastatic OSCC.

HuMax-IL8 is a fully human monoclonal antibody developed to neutralize IL-8-mediated biological activities, including tumor progression, immune evasion, epithelial–mesenchymal transition, and recruitment of myeloid-derived suppressor cells (Bilusic et al. 2019). In a phase I clinical trial involving patients with metastatic or unresectable solid tumors, HuMax-IL8 treatment was well tolerated and resulted in disease stabilization accompanied by reduced circulating IL-8 levels (Bilusic et al. 2019). These clinical observations, together with our findings demonstrating that IL-8 sustains NF-κB activation through a positive feedback mechanism in OSCC, highlight the potential therapeutic relevance of targeting the IL-8/NF-κB signaling axis in metastatic disease. Consistent with the clinical importance of IL-8 signaling, elevated circulating IL-8 levels have been associated with poor responses to immune checkpoint blockade in patients with head and neck cancer, melanoma, renal cell carcinoma, and unresectable hepatocellular carcinoma (Zhang et al. 2024; Schalper et al. 2020). Furthermore, recent evidence suggests that simultaneous inhibition of IL-8 and programmed death-ligand 1 (PD-L1) pathways may provide a promising therapeutic approach for triple-negative breast cancer, an aggressive malignancy characterized by high metastatic potential (Dominguez et al. 2017). In addition, reduced salivary IL-8 levels in patients with head and neck cancer before radiotherapy have been correlated with improved treatment outcomes (Principe et al. 2022). Together, these findings raise the possibility that IL-8 inhibition, alone or in combination with radiotherapy or immunotherapy, may represent a potential therapeutic strategy for OSCC patients with elevated IL-8 expression. Future studies are warranted to determine whether HuMax-IL8-based combination therapies can overcome metastatic progression or radioresistance in OSCC.

Conclusions

Our study identifies IL-8 as a critical mediator of lymph node metastatic progression in OSCC. We demonstrate that IL-8 activates CXCR1/2-dependent NF-κB signaling, which subsequently reinforces IL-8 expression, establishing a positive feedback loop that maintains the metastatic phenotype of OSCC cells. Pharmacological disruption of this signaling circuit effectively attenuates the migratory and metastatic properties of OSCC cells with elevated IL-8 expression. These findings highlight IL-8 as a potential biomarker for identifying OSCC patients at increased risk of lymph node metastasis and provide a translational rationale for targeting the IL-8–CXCR1/2–NF-κB signaling axis as a therapeutic strategy for metastatic OSCC.

Abbreviations

OSCC
Oral squamous cell carcinoma
TCGA
IL-8:Interleukin-8
The Cancer Genome Atlas
GEO
Gene Expression Omnibus

JCRB
Japanese Collection of Research Bioresources
RT-PCR
Reverse transcription-polymerase chain reaction
Q-PCR
Quantitative PCR
GSEA
Gene Set Enrichment DEGs:Analysis
differentially expressed genes
PD-L1
Programmed death-ligand 1.

Declarations

Acknowledgements

The Fig. 7 were created with https://BioRender.com.

Authors' contributions

Y.F.L., S.W.F. and H.L.L designed and coordinated the project. Y.F.L and H.L.L performed the experiments and drafted the manuscript. S.W. F. modified the manuscript and provided valuable advice. C.H.L., H.W.L. and Y.H.K.L. helped perform the experiments and modify the manuscript during revision stage. S.D.Y., I.C.L. and C.B.H. helped the designation of experiments and analyzed the data. C.H.L. and H.W.L. helped the collection of tissue sample. All authors read and approved the final manuscript.

Funding

This work was supported by Taipei Medical University Hospital (111TMU-TMUH-03-4) and National Science and Technology Council, Taiwan (NSTC 114-2320-B-038 -041 -MY3 to Yuan-Feng Lin and NSTC 114-2628-B-038-003-MY3 to Hsin-Lun Lee).

Data availability

The data that supports the findings of this study are available from the corresponding author upon reasonable request.

Ethics approval

Primary tumors and normal adjacent tissues of OSCC patients were obtained from Taipei Medical University Biobank and collected with institutional review board approval (N202204007) and the Declaration of Helsinki.

Consent to participate declaration

Not applicable.

Consent for publication

All authors have agreed with publishing this manuscript.

Competing interests

The authors declare no competing interests.

References

1. Abrahao R, Perdomo S, Pinto LFR, Nascimento de CF, Dias FL, de Podesta JRV, von Ventorin AP, Vilensky M, Giglio RE, Oliveira JC, Mineiro MS, Kowalski LP, Ikeda MK, Cuello M, Munyo A, Rodriguez-Urrego PA, Hakim JA, Suarez-Zamora DA, Cayol F, Figari MF, Oliver J, Gaborieau V, Keogh RH, Brennan P, Curado MP. Predictors of Survival After Head and Neck Squamous Cell Carcinoma in South America: The InterCHANGE Study. JCO Glob Oncol. 2020;6:486–99.
2. Bilusic M, Heery CR, Collins JM, Donahue RN, Palena C, Madan RA, Karzai F, Marte JL, Strauss J, Gatti-Mays ME, Schlom J, Gulley JL. Phase I trial of HuMax-IL8 (BMS-986253), an anti-IL-8 monoclonal antibody, in patients with metastatic or unresectable solid tumors. J Immunother Cancer. 2019;7:240.
3. Dominguez C, McCampbell KK, David JM, Palena C. Neutralization of IL-8 decreases tumor PMN-MDSCs and reduces mesenchymalization of claudin-low triple-negative breast cancer. JCI Insight 2017;2.
4. El-Sakka H, Kujan O, Farah CS. Assessing miRNAs profile expression as a risk stratification biomarker in oral potentially malignant disorders: A systematic review. Oral Oncol. 2018;77:57–82.
5. Gamboa A, Gronchi A, Cardona K. Soft-tissue sarcoma in adults: An update on the current state of histiotype-specific management in an era of personalized medicine. CA Cancer J Clin. 2020;70:200–29.
6. Gupta S, Tomar A, Singh R. Personalized medicine in oral cancer. Crit Rev Oncol Hematol. 2025;209:104670.
7. Han XQ, Qi ZL, He L, Lu D, Zhao T. Touch-down PCR and single-strand conformation polymorphism for detecting clonal T cell receptor gamma gene rearrangement in lymphoid leukemia. Di Yi Jun Yi Da Xue Xue Bao. 2004;24:188–91.
8. Hedges JC, Singer CA, Gerthoffer WT. Mitogen-activated protein kinases regulate cytokine gene expression in human airway myocytes. Am J Respir Cell Mol Biol. 2000;23:86–94.
9. Jeong Y, Yoon SY, Jung SP, Nam SJ, Lee JE, Kim S. Inhibition of Interleukin-8/C-X-C Chemokine Receptor 2 Signaling Axis Prevents Tumor Growth and Metastasis in Triple-Negative Breast Cancer Cells. Pharmacology. 2025;110:178–90.

10. Joshi S, Pandey R, Kumar A, Gupta V, Arya N. Targeted blockade of interleukin-8 negates metastasis and chemoresistance via Akt/Erk-NFkappaB axis in oral cancer. Cytokine. 2023;166:156155.
11. Kumar P, Singh K, Garg A, Urs AB, Augustine J, Salivary. IL-8, CYFRA 21 – 1, and CD44 for early detection of oral squamous cell carcinoma: a systematic review and meta-analysis. Clin Chim Acta. 2025;577:120471.
12. Li P, Chen X, Qin G, Yue D, Zhang Z, Ping Y, Wang D, Zhao X, Song M, Zhao Q, Li J, Liu S, Wang D, Zhang C, Lian J, Cao L, Li F, Huang L, Wang L, Yang L, Huang J, Li H, Zhang B, Zhang Y. Maelstrom Directs Myeloid-Derived Suppressor Cells to Promote Esophageal Squamous Cell Carcinoma Progression via Activation of the Akt1/RelA/IL8 Signaling Pathway. Cancer Immunol Res. 2018;6:1246–59.
13. Lin HY, Wang WK, Lin CH, Kuei CH, Lee HH, Kent Lin YH, Chiu HW, Lin YF. The IL-8/NF-kappaB feedback loop confers a paclitaxel-sensitive/doxorubicin-resistant phenotype in triple-negative breast cancer. Free Radic Biol Med. 2025;238:316–28.
14. Mizuno M, Nakano R, Nose S, Matsumura M, Nii Y, Kurogochi K, Sugiya H, Uechi M. Canonical NF-kappaB p65, but Not p105, Contributes to IL-1beta-Induced IL-8 Expression in Cardiac Fibroblasts. Front Immunol. 2022;13:863309.
15. Oem JK, Jackel-Cram C, Li YP, Kang HN, Zhou Y, Babiuk LA, Liu Q. Hepatitis C virus non-structural protein-2 activates CXCL-8 transcription through NF-kappaB. Arch Virol. 2008;153:293–301.
16. Park JY, Chang JH, Bae KS, Lee KH, Choi SJ, Park JY, Ryang YS, Kim SK. NF-kappaB-dependency and consequent regulation of IL-8 in echinomycin-induced apoptosis of HT-29 colon cancer cells. Cell Biol Int. 2008;32:1207–14.
17. Peng CY, Wang TY, Lee SS, Hsieh PL, Liao YW, Tsai LL, Fang CY, Yu CC, Hsieh CS. Let-7c restores radiosensitivity and chemosensitivity and impairs stemness in oral cancer cells through inhibiting interleukin-8. J Oral Pathol Med. 2018;47:590–7.
18. Peng HY, Jiang SS, Hsiao JR, Hsiao M, Hsu YM, Wu GH, Chang WM, Chang JY, Jin SL, Shiah SG. IL-8 induces miR-424-5p expression and modulates SOCS2/STAT5 signaling pathway in oral squamous cell carcinoma. Mol Oncol. 2016;10:895–909.
19. Principe S, Zapater-Latorre E, Arribas L, Garcia-Miragall E, Bagan J. Salivary IL-8 as a putative predictive biomarker of radiotherapy response in head and neck cancer patients. Clin Oral Investig. 2022;26:437–48.
20. Pu Y, Li Q, Wang Y, Xu L, Qiao Q, Guo Y, Guo C. pERK-mediated IL8 secretion can enhance the migration, invasion, and cisplatin resistance of CD10-positive oral cancer cells. BMC Cancer. 2021;21:1283.
21. Sahibzada HA, Khurshid Z, Khan RS, Naseem M, Siddique KM, Mali M, Zafar MS. Salivary IL-8, IL-6 and TNF-alpha as Potential Diagnostic Biomarkers for Oral Cancer. Diagnostics (Basel) 2017;7.
22. Sanmamed MF, Perez-Gracia JL, Schalper KA, Fusco JP, Gonzalez A, Rodriguez-Ruiz ME, Onate C, Perez G, Alfaro C, Martin-Algarra S, Andueza MP, Gurpide A, Morgado M, Wang J, Bacchiocchi A, Halaban R, Kluger H, Chen L, Sznol M, Melero I. Changes in serum interleukin-8 (IL-8) levels reflect

and predict response to anti-PD-1 treatment in melanoma and non-small-cell lung cancer patients. Ann Oncol. 2017;28:1988–95.

23. Schalper KA, Carleton M, Zhou M, Chen T, Feng Y, Huang SP, Walsh AM, Baxi V, Pandya D, Baradet T, Locke D, Wu Q, Reilly TP, Phillips P, Nagineni V, Gianino N, Gu J, Zhao H, Perez-Gracia JL, Sanmamed MF, Melero I. Elevated serum interleukin-8 is associated with enhanced intratumor neutrophils and reduced clinical benefit of immune-checkpoint inhibitors. Nat Med. 2020;26:688–92.
24. Song Y, Li Y, Zhou J, Yu J, Hu Q, Yang F, Yin Z, Wang Y, Wang Y, Zhang X, Tao Y, Peng C, Liu S. IL-8-NF-kappaB-ALDH1A1 loop promotes the progression of intrahepatic cholangiocarcinoma. Hepatol Commun 2025;9.
25. Speight PM, Khurram SA, Kujan O. Oral potentially malignant disorders: risk of progression to malignancy. Oral Surg Oral Med Oral Pathol Oral Radiol. 2018;125:612–27.
26. Tamatani T, Azuma M, Ashida Y, Motegi K, Takashima R, Harada K, Kawaguchi S, Sato M. Enhanced radiosensitization and chemosensitization in NF-kappaB-suppressed human oral cancer cells via the inhibition of gamma-irradiation- and 5-FU-induced production of IL-6 and IL-8. Int J Cancer. 2004;108:912–21.
27. Xu ZP, Song Y, Yang K, Zhou W, Hou LN, Zhu L, Chen HZ, Cui YY. M3 mAChR-mediated IL-8 expression through PKC/NF-kappaB signaling pathways. Inflamm Res. 2014;63:463–73.
28. Zeng G. Sticky-end PCR: new method for subcloning. Biotechniques. 1998;25:206–8.
29. Zhang J, Yin Y, Tang J, Zhang Y, Tian Y, Sun F. Changes in Serum Interleukin-8 Levels Predict Response to Immune Checkpoint Inhibitors Immunotherapy in Unresectable Hepatocellular Carcinoma Patients. J Inflamm Res. 2024;17:3397–406.

Figures

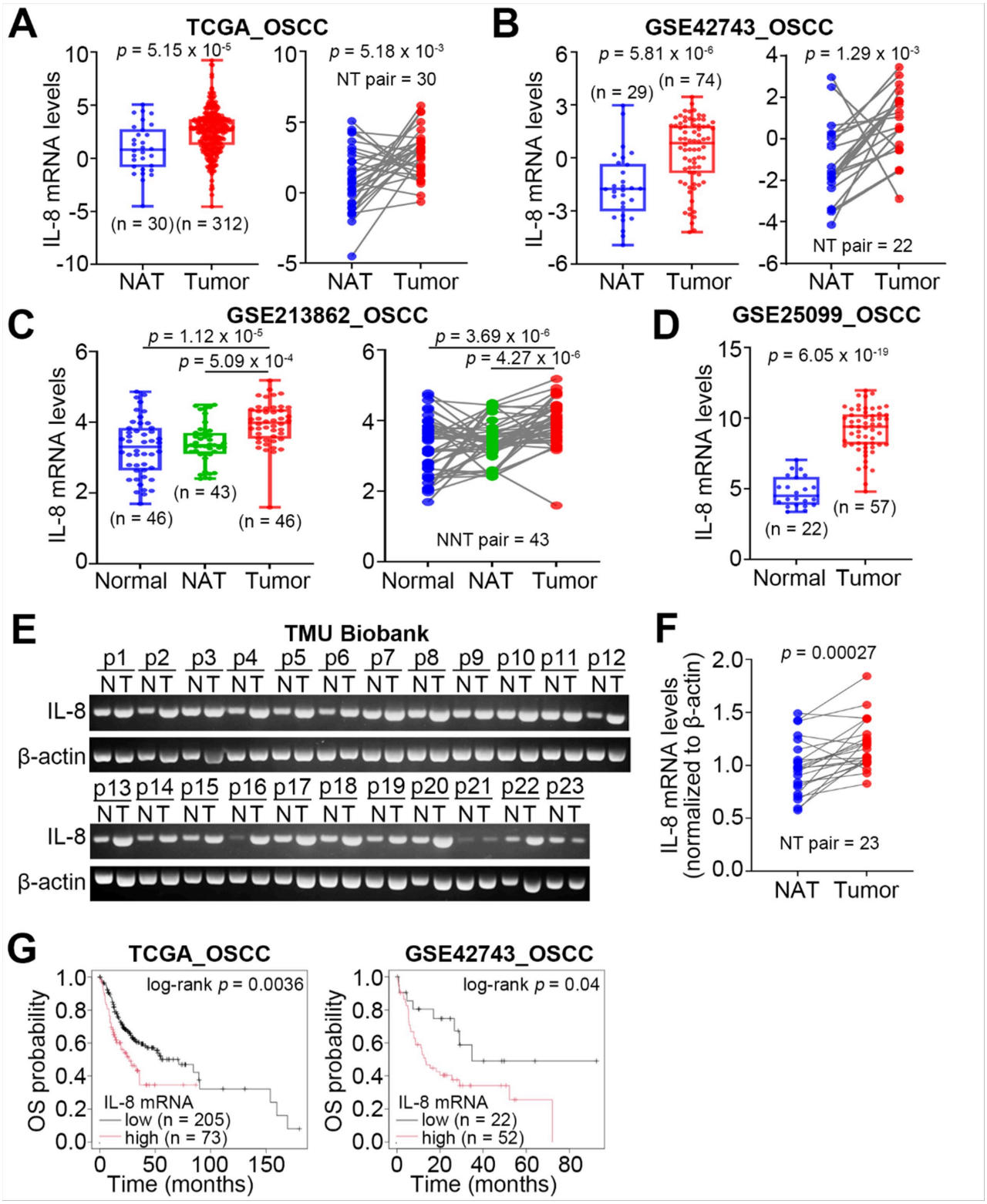


Figure 1

IL-8 upregulation is commonly detected in primary tumors compared to adjacent normal tissues and refers to a poor prognostic biomarker in oral squamous cell carcinoma. **A – D** Box plots and dotted line plots for the IL-8 mRNA levels in normal oral cavity tissues from healthy donors, as well as normal adjacent tissues (NATs) and primary tumors from OSCC patients in the TCGA, GSE42743, GSE213862, and GSE25099 datasets. **E** RT-PCR analysis and **F** dotted line plots of IL-8 mRNA levels in paired normal

adjacent tissues (N) and primary tumors (T) from 23 OSCC patients obtained from the Taipei Medical University (TMU) Biobank. b-actin was used as an internal control of experiment. **G** Kaplan–Meier survival analyses of IL-8 mRNA expression under a maximal risk condition using overall survival (OS) probability against TCGA (left) and GSE42743 (right) OSCC patients.

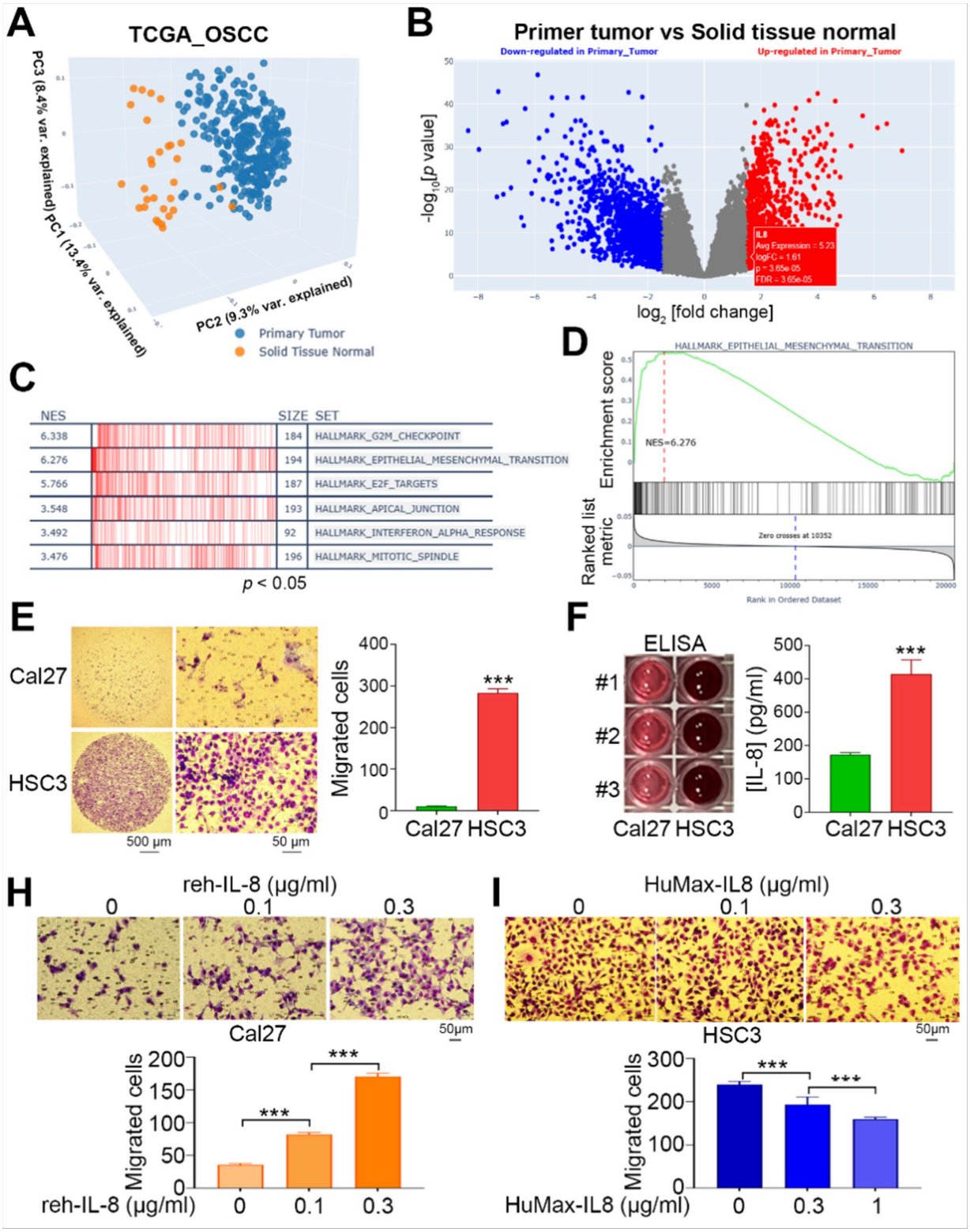


Figure 2

IL-8 upregulation associates with an enhanced migration ability of OSCC cells. **A** Principal component analysis (PCA) of transcriptional profiles from solid tissue normal samples (normal adjacent tissues) and primary tumors, and **B** a volcano plot showing differential gene expression between primary tumors and solid tissue normal samples from TCGA OSCC patients. **C** List of activated pathways from Hallmark gene sets and **D** enrichment score plot of the epithelial–mesenchymal transition gene set, generated by GSEA using a gene list ranked by fold change as shown in (**B**). NES is the abbreviation of normalized enrichment score (**C**). SIZE and SET represent the gene number of dataset and the name of Hallmark gene sets. **E** Cell migration assays, visualized by Giemsa staining (left) and quantified by bar charts (right) after trans-well cultivation for 8 hours, and **F**ELISA measurement of extracellular IL-8 levels, presented as colorimetric images (left) and quantified by bar charts (right) in Cal27 and HSC3 cells. (H and I) **H, I** Giemsa staining (upper) and corresponding quantification (lower) of migrated cells in trans-well assays of Cal27 cells treated with recombinant human IL-8 (rhIL-8) at the indicated concentrations, and HSC3 cells treated with or without the humanized IL-8–neutralizing antibody HuMax-IL8 at the indicated concentrations. *** denotes the statistical significance at $p < 0.001$ (**E – I**).

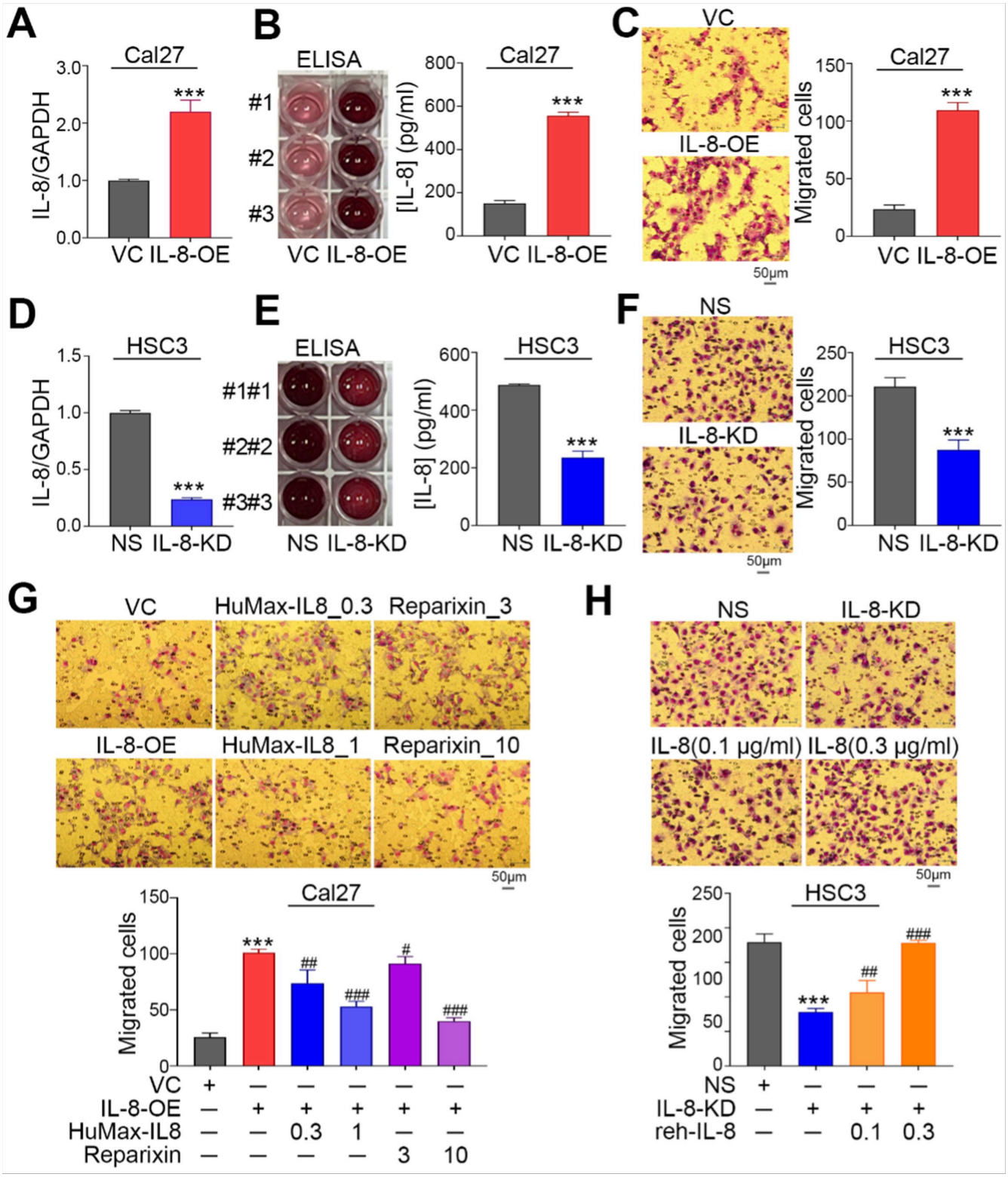


Figure 3

IL-8 acts as a driver in promoting the metastatic potentials of OSCC. **A – F**IL-8 mRNA expression quantified by qPCR, extracellular IL-8 levels measured by ELISA and presented as colorimetric images (left) with corresponding quantification (right), and cell migration assays visualized by Giemsa staining (left) and quantified by bar charts (right) following trans-well assays in vector control (VC) and IL-8–overexpressing (OE) Cal27 cells, as well as non-silencing (NS) control and IL-8–knockdown (KD) HSC3

cells. **G, H** Giemsa staining (upper) and corresponding quantification (lower) of migrated cells in trans-well assays of VC and IL-8–OE Cal27 cells pretreated with or without HuMax-IL8 or the IL-8 receptor (CXCR1/2) antagonist Reparixin at the indicated concentrations, and NS control and IL-8–KD HSC3 cells cultured in the absence or presence of reh-IL-8 at the indicated concentrations. *** denotes the statistical significance at $p < 0.001$ (**A – F**). *** indicates statistical significance at $p < 0.001$ compared with the VC and NS control groups, whereas #, ##, and ### indicate statistical significance at $p < 0.05$, $p < 0.01$, and $p < 0.001$, respectively, compared with the IL-8-OE and IL-8-KD groups (**G, H**).

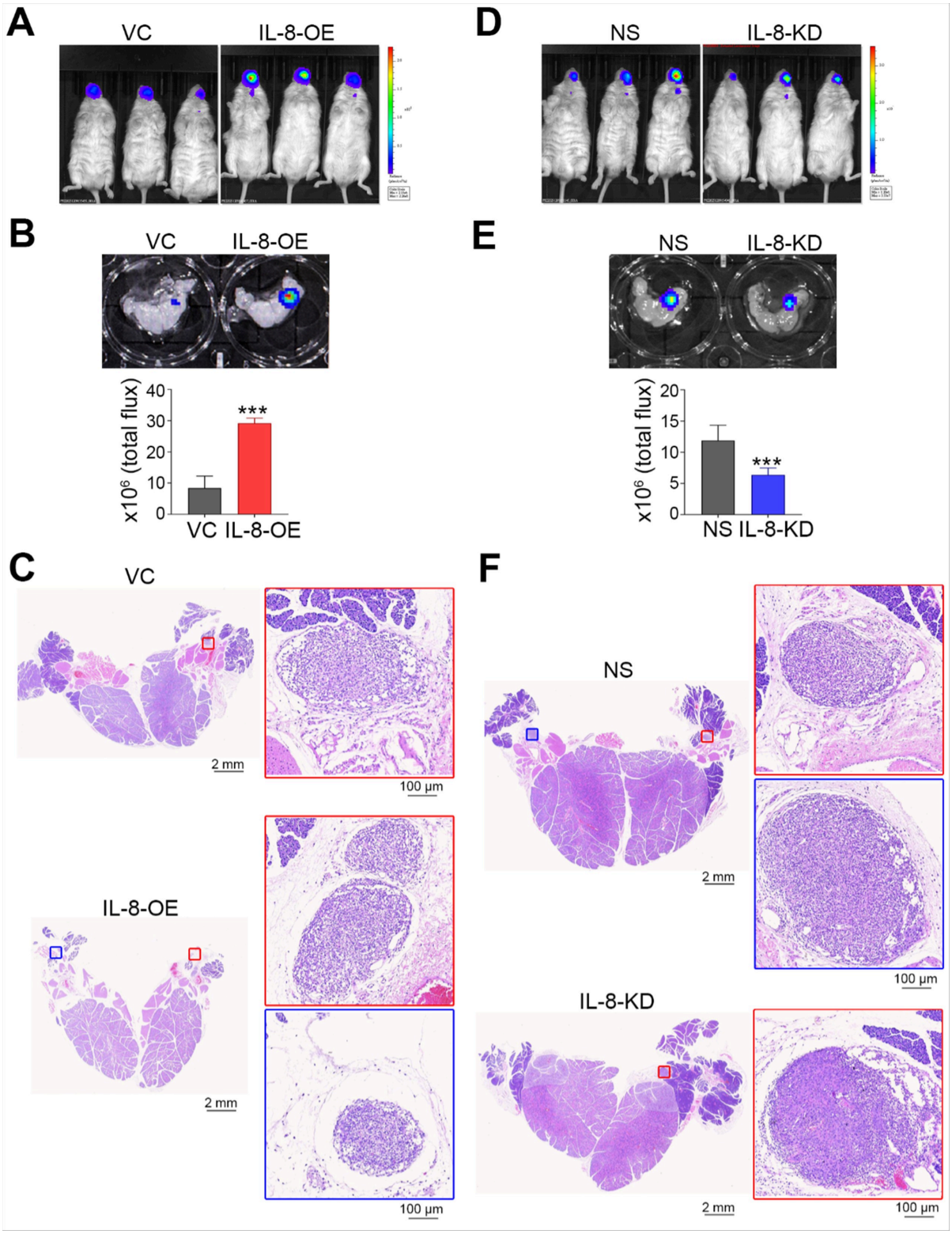


Figure 4

IL-8 expression causally associates with the lymph node metastatic capacity of OSCC cells. **A – F** Bioluminescent imaging of luciferase-expressing OSCC cells in tumor-bearing mice; cervical tissues showing representative images (upper) with corresponding quantification of photon flux presented as bar charts (lower); and H&E staining of lymph nodes from mice implanted with luciferase-labeled VC/IL-8–OE Cal27 cells or NS/IL-8–KD HSC3 cells. *** denotes the statistical significance at $p < 0.001$ (**B, E**).

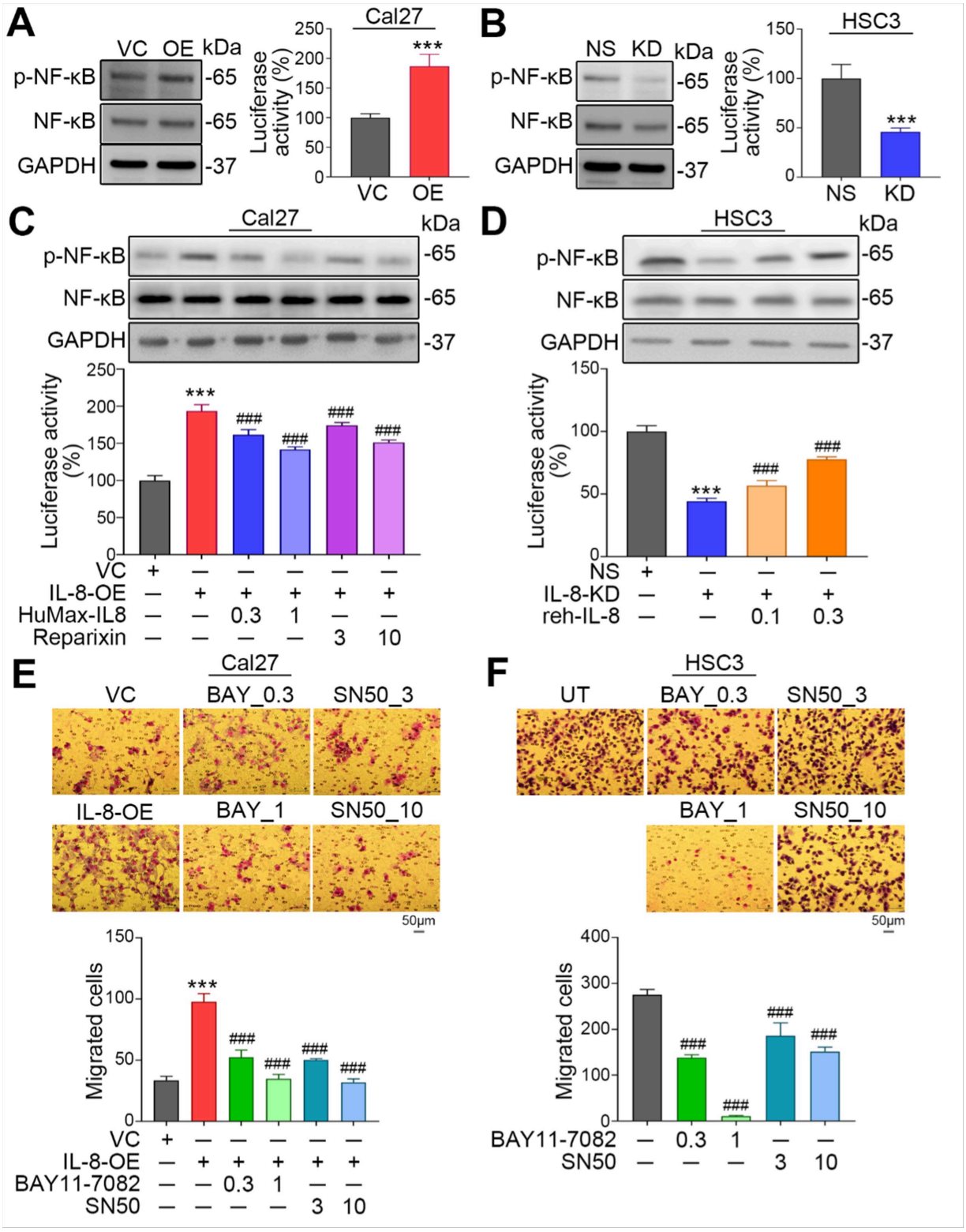


Figure 5

IL-8 promotes cellular migration through receptor engagement and NF-κB activation in OSCC cells. **A, B** Western blot analyses of phosphorylated NF-κB (p-NF-κB), total NF-κB, and GAPDH (left), together with NF-κB–dependent luciferase reporter activity (right), in VC and IL-8–OE Cal27 cells or NS control and IL-8–KD HSC3 cells. **C, D** Western blot analyses of p-NF-κB, total NF-κB, and GAPDH (upper), and corresponding NF-κB luciferase reporter activity (lower), in VC and IL-8–OE Cal27 cells pretreated with or without HuMax-IL8 or Reparixin at the indicated concentrations, or in NS control and IL-8–KD HSC3 cells cultured in the absence or presence of rehIL-8 at the indicated concentrations. **E, F** Giemsa staining (upper) and corresponding quantification (lower) of migrated cells in trans-well assays of VC and IL-8–OE Cal27 cells pretreated with the NF-κB inhibitors BAY11-7082 (BAY) or SN50 at the indicated concentrations, and HSC3 cells treated with both NF-κB inhibitors at the indicated concentrations. *** indicates statistical significance at $p < 0.001$ compared with the VC and NS groups, whereas ### indicates statistical significance at $p < 0.001$ compared with the IL-8-OE and IL-8-KD groups (**A – E**). ### indicates statistical significance at $p < 0.001$ compared with the untreated group (**F**).

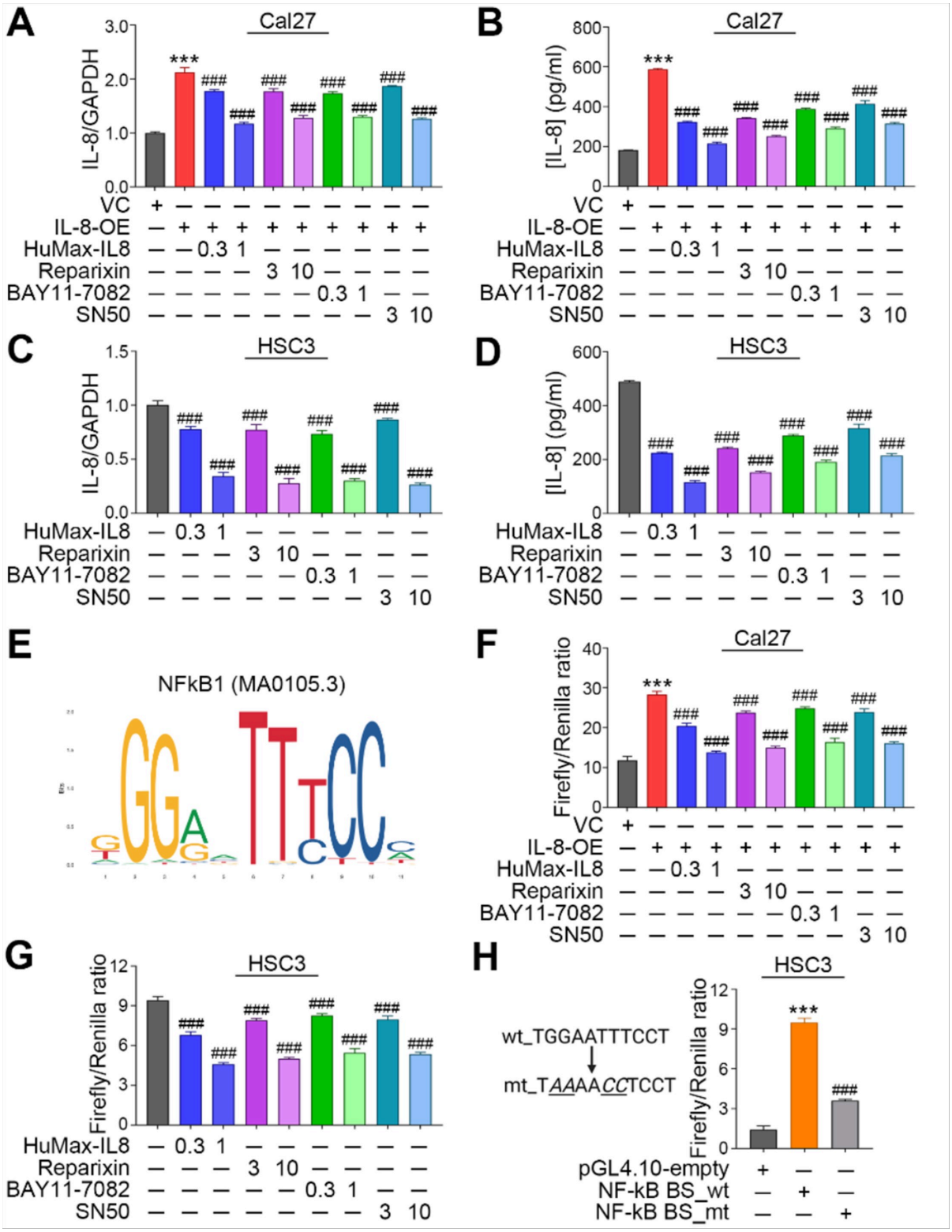


Figure 6

IL-8 forms a positive feedback loop through receptor engagement and NF-κB activation in OSCC cells. **A – D** Quantification of IL-8 expression, shown as IL-8 mRNA levels determined by qPCR and extracellular IL-8 protein levels measured by ELISA, in VC and IL-8–OE Cal27 cells and HSC3 cells treated with or without HuMax-IL8, Reparixin, BAY11-7082 or SN50 at the indicated concentrations. **E** Sequence logo depicting the predicted nucleotide frequency of the NF-κB (NFKB1) binding motif identified in the IL-8

promoter region (−91 to −82 bp) based on the JASPAR database. **F, G** IL-8 promoter–driven luciferase reporter assays, shown as normalized firefly luciferase activity relative to Renilla luciferase activity, in VC and IL-8–OE Cal27 cells and HSC3 cells treated with or without HuMax-IL8, reparixin, BAY11-7082, or SN50 at the indicated concentrations. **H** Schematic representation of the predicted NF-κB binding sites within the IL-8 promoter, showing wild-type (wt) and mutant (mt) sequences (italicized and underlined) (left), and corresponding luciferase reporter activity in HSC3 cells transfected with the pGL4.10 empty vector or pGL4.10 constructs containing the IL-8 promoter region (−1 to −1000 bp) with or without mutation of the NF-κB binding site (right). *** indicates statistical significance at $p < 0.001$ compared with the VC groups, whereas ### indicates statistical significance at $p < 0.001$ compared with the IL-8-OE and untreated groups (**A – D, F, G**). *** indicates statistical significance at $p < 0.001$ compared with the pGL4.10 empty vector groups, whereas ### indicates statistical significance at $p < 0.001$ compared with the NF-κB BS_wt groups (**H**).

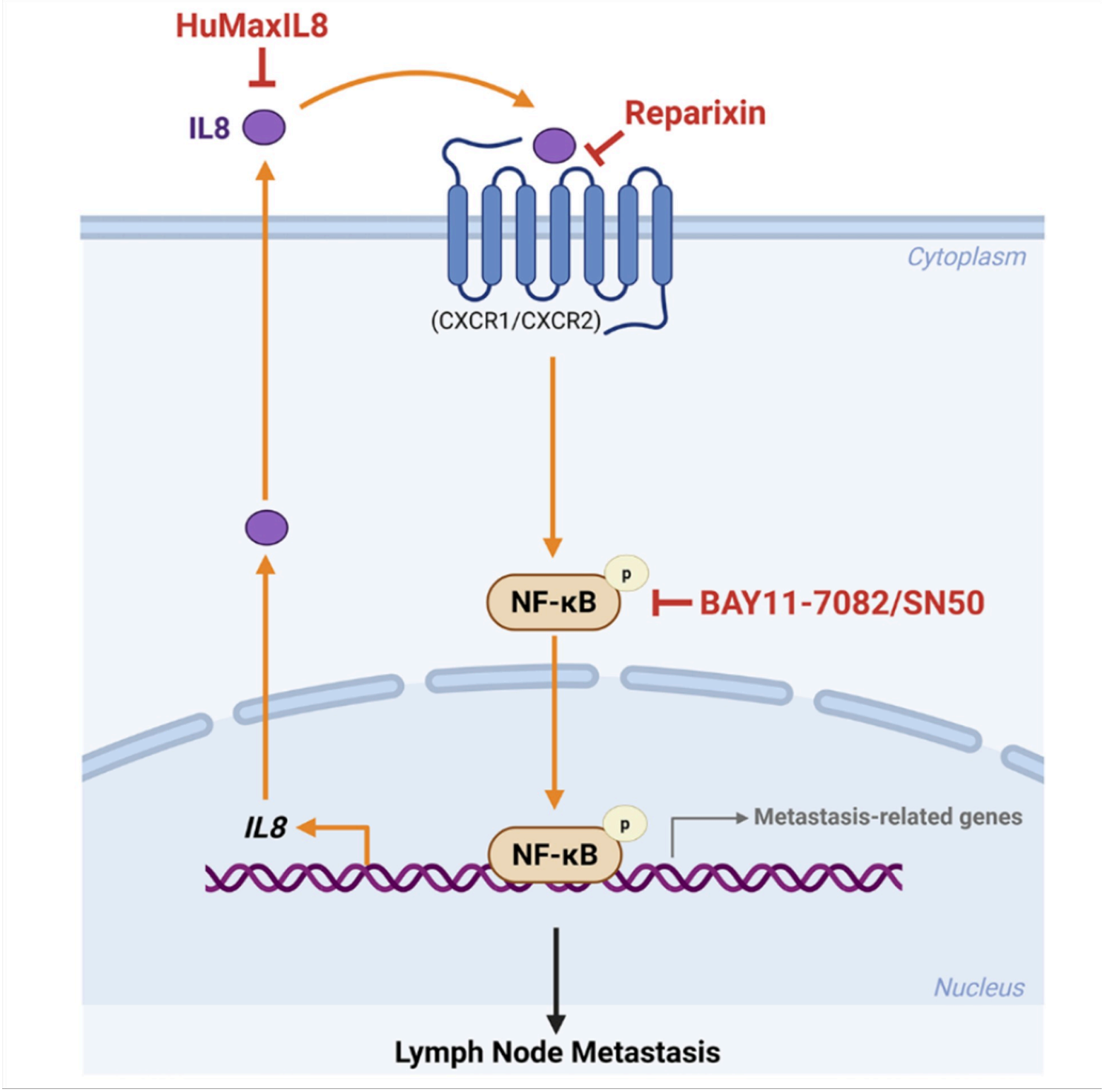


Figure 7

Proposed model illustrating how the IL-8/NF-κB positive feedback loop drives lymph node metastasis in OSCC. Upregulated IL-8 induces receptor engagement and NF-κB activation, thereby establishing a positive feedback loop that ultimately enhances the lymph node metastatic capacity of OSCC cells. Targeting this feedback loop using the humanized IL-8–neutralizing antibody HuMax-IL8, the IL-8 receptor (CXCR1/2) antagonist Reparixin, or NF-κB–specific inhibitors (e.g., BAY11-7082 or SN50) may represent a potential therapeutic strategy for metastatic OSCC with elevated IL-8 expression.

Supplementary Files

This is a list of supplementary files associated with this preprint. Click to download.

- ThefulluncroppedGelsandBlotsimages.docx
- SupplementaryInformation.docx